Imaging Properties Of A Metamaterial Superlens

Nicholas Fang and Xiang Zhang

Department of Mechanical and Aerospace Engineering, University of California at Los Angeles, 420 Westwood Plaza, Los Angeles, CA 90095, USA

Abstract — **The subwavelength imaging quality of a metamaterial superlens is studied numerically in wavevector domain. Examples of image compression and magnification are given and resolution limits are discussed. A minimal resolution of λ/6 is obtained using 36nm siver film at 364nm wavelength. Simulation also demonstrates the power flux is no longer a good measure to determine the focal plane of superlens due the elevated field strength at exit side of metamaterial slab.**

I. Introduction

Meta-materials have opened an exciting gateway to reach unprecedented physical properties and functionality unattainable from naturally existing materials. The "atoms" and "molecules" in meta-materials can be tailored in shape and size, the lattice constant and inter-atomic interaction can be artificially tuned, and "defects" can be designed and placed at desired locations. Pioneering work on strongly modulated photonic crystals [1] represent a giant step in engineered meta-materials. The recent discovery of left-handed meta-materials(LHM) [2,3] with negative effective permittivity and permeability over a designed frequency band is an excellent example of new exciting physics arising from meta-materials. A medium of this type was speculated "left-handed" originally by Veselago[4], because for an electromagnetic plane wave propagating inside the LHM, the direction of Poynting vector is opposite to that of wavevector.

Veselago suggested in his original paper a rectangular slab of LHM could focus the electromagnetic radiation. Very recently, Pendry[5] predicted an intriguing property of such a LHM lens: unlike conventional optical components, it will focus both the propagating spectra as well as the evanescent waves, thus capable of achieving diffraction-free imaging. From quasi-static theory, Pendry further suggested that for near-field imaging, the permittivity and permeability of the meta-material can be designed independently in accordance to TM and TE polarization, respectively. For example, a negative value of permittivity can be observed in a thin metal film. In this case, the film will be able to image the TM waves of the near-field object to the opposite side, with a resolution significantly below the diffraction limit.

However, Pendry's quasi-static theory did not address the following questions: How the loss and dielectric mismatch affects the imaging quality? Is it possible to generate reduction or magnification with LHM? What is a good measure of the depth of focus in the superlens? In this paper, we are going to present the numerical results in attempt to answer these questions.

II. Theory and Modeling

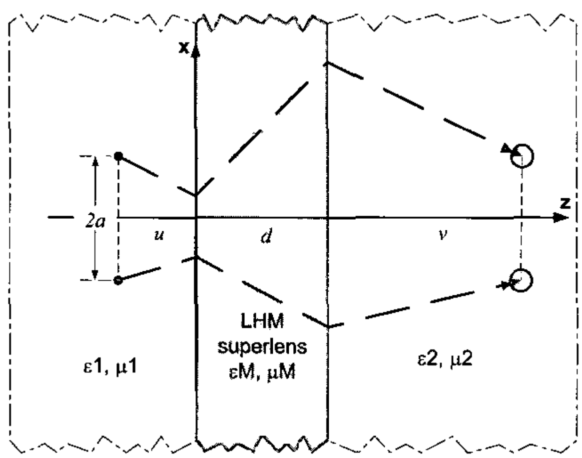

Fig. 1 The model of a LHM lens under the radiation of two line current sources.

Fig. 1 depicts the 2D imaging system in our study. For simplicity without loss of generality, here we consider the imaging quality of two monochromatic line current sources transmitted through a meta-material slab of thickness d, located between z=0 and z=d. The sources are embedded in medium 1 with uniform and isotropic permittivity ε_1 and permeability μ_1, displaced by width $2a$, and the separation from sources to the slab is defined the object distance u. The light field due to the TM sources $\vec{J}(\mathbf{r}) = \hat{z}I\delta(\mathbf{r}-\mathbf{r}')$, located at $\mathbf{r}' = (x = \pm a, z = -u)$ is propagating through the meta-lens with designed properties ε_m and μ_m, and transmitted to medium 2 where the images are formed at distance v to the lens.

The imaging capability associated with the left-hand meta-material slabs is based on the effect of negative refraction [4-6]. From paraxial-ray treatment in geometric optics, the refracted wave from the object will converge first inside the slab and produces a 2D image by transformation: (x, y, -u) $\rightarrow$ (x, y, $|n_M/n_1|$u), and as the waves advance to reach the other interface of the slab, negative refraction occurs again to produce a second image in the half space of medium 2, located at (x, y, $(1+|n_2/n_M|)d-|n_M/n_1|u$). Therefore, paraxial analysis predict that the image produced by a slab metalens is characterized by $v=|n_2/n_M|d-|n_M/n_1|u$.

The image quality of this model system can be characterized using the conventional optical transfer function(OTF), defined by the ratio of image field over original object field H_{img}/H_{obj} with given lateral component of wavevector k_x. From Fresnel's formula of the stratified medium, the optical transfer function of the meta-lens can now be written as

$$OTF(k_x) = \frac{t_{1M}t_{M2}\exp(i\beta_M d)\exp(i\beta_1 u)\exp(i\beta_2 v)}{1+r_{1M}r_{M2}\exp(2i\beta_M d)}, \quad (1)$$

where $\beta_M = \sqrt{\varepsilon_M\mu_M\varepsilon_0\mu_0\left(\frac{\omega}{c}\right)^2 - k_x^2}$, and t and r are Fresnel coefficient of transmission and reflection at interfaces indicated by subscriptions. Please note that for a perfect imaging system, the OTF should remain constant regardless the variation of k_x.

In order to find the imaging properties, we can now decompose the incident object field $\vec{H}_{obj}$ at (-u<z<0) impressed by the object into superposition of lateral components with the help of Weyl integral:

$$\vec{H}_{obj}(x,-u<z<0) = \frac{\nabla\times\hat{z}}{4\pi}\int_{-\infty}^{\infty} dk_x \frac{\exp(ik_x x + i\beta_1|z+u|)}{i\beta_1} I(k_x,\beta_1), \quad (2)$$

where $I(k_x,\beta_1)$ represents the Fourier transformed part of line current source $I\delta(\mathbf{r}-\mathbf{r}')$.

As a result, the image field at focal point $z=d+v$ is simply the convolution of the source field and the OTF:

$$\vec{H}_{img}(x,z=d+v) = \frac{\nabla\times\hat{z}}{4\pi}\int_{-\infty}^{\infty} dk_x \frac{\exp(ik_x x)}{i\beta_1} I(k_x) OTF(k_x). \quad (3)$$

III. Enhanced Transmission Of Evanescence

A key function of the metamaterial superlens is to transmit the lateral field component of object at large spatial frequency k_x with enhanced amplitude. In symmetrical case($\varepsilon_1=\varepsilon_2=1$, $\mu_1=\mu_2=1$), the TM transmission coefficient reads as following:

$$T_P = \frac{4\varepsilon_M\beta_1\beta_M}{(\varepsilon_M\beta_1+\beta_M)^2\exp(-i\beta_M d)-(\varepsilon_M\beta_1-\beta_M)^2\exp(i\beta_M d)}. \quad (4)$$

We can now define two operators L^+ and L^-[7]:

$$L^+ = \varepsilon_M\beta_1 + \beta_M\tanh\left(\frac{\beta_M d}{2i}\right); \quad (5a)$$

$$L^- = \varepsilon_M\beta_1 + \beta_M\coth\left(\frac{\beta_M d}{2i}\right); \quad (5b)$$

and the transmission function is simply

$$T_P = \frac{2\varepsilon_M\beta_1\beta_M}{L^+L^-\sinh\frac{\beta_M d}{i}} = 2\varepsilon_M\beta_1\left(\frac{1}{L^+}-\frac{1}{L^-}\right) \quad (6)$$

Thus, for large k_x and $\varepsilon_M \neq -1$, the transmission off resonance reads:

$$T_P \approx \frac{8\varepsilon_M\beta_1\beta_M}{(\varepsilon_M\beta_1+\beta_M)^2}\exp(i\beta_M d) \approx \frac{8\varepsilon_M}{(\varepsilon_M+1)^2}\exp(-|k_x|d) \quad \ldots\ldots (7).$$

It can be seen from Eq(7) that the transmission decays exponentially with increasing thickness d. Thus for a large mismatch ($|\delta\varepsilon|>1$) the resolution limit as a rule of thumb is ~ $2d$. On the other hand, when the surface resonance occurs (L^+ or L^- $\rightarrow$0), the transmission is at local maximum. Therefore, the field components near resonance are disproportionably enhanced in the resulting image [9].

III. Simulation Results And Discussion

Although left-handed metamaterials are now realized in microwave range, essential engineering methods have to be developed in order to meet the critical demand of desired values of ε and μ towards a functioning superlens. As an initial effort, we focus on the negative ε properties since this is the only relevant material response to TM light in electrostatic limit. To illustrate the sensitivity of image resolution dependence on the material properties mismatch, in Fig. 2 we plot the modulation transfer function ($|OTF|^2$) of a metamaterial superlens due to mismatch of ε. It is clear that in order to achieve high spatial resolution (>λ/10) in superlens, the controllability of ε_M should be better than 1%. More interestingly, the cutoff of spatial resolution always follows the resonant peak due to excitation of surface waves described by Eqs(5a,b). As a practical rule, we can locate these peaks as a guideline of the cutoff spatial frequency. In quasi-static limit, the peaks can be predicted by $k_{x,max}/k_0=\lambda log(2/|\delta\varepsilon|)/2\pi d$. This is in good agreement with our simulation, as shown in the inset of Fig. 2. Furthermore, it turns out the effect of loss characterized by the imaginary part of ε can also be approximated in this equation. In the case of Imag(ε)=0.4, the result is approximately 2.6, indicating a resolution of ~λ/3.

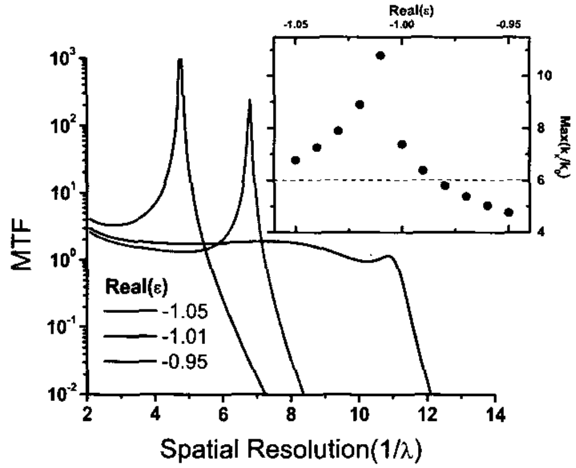

Fig. 2 The modulation transfer function (MTF) of a LHM superlens exhibits lower cutoff due to mismatch of ε. The thickness d of the lens is λ/10, with μ=1, Imag(ε)=0.001.The inset depicts the displacement of surface resonance peak as a function of mismatch of ε.

It is clear from the above discussion that to further improve the resolution limit in superlens, we have to consider a surrounding medium with dielectric function ε>1. For instance, we select medium 1 to be glass (ε_1=2.368), and medium 2 to be photoresist (ε_2=2.79). In this case we are facing a slightly asymmetric condition, with Imag(ε_M)=0.27. The simulation result of average Poynting vector |Real(S(x,z))| at paraxial focal plane z=d+v is shown in Fig. 3. It can be found that a resolution of λ/6 is achieved at Real(ε_M)=-2.4, which correspond to 364nm wavelength. In addition, when ε is tuned to more negative values, we obtain a compressed image(Real(ε_M)= -3.0 case in Fig. 3). In contrast, a expanded image is observable at less negative ε. Unlike the magnification or demagnification in conventional optics, these phenomena are attributed to the contribution of surface resonances which detuned the lateral peak width[10] and position. This argument can be justified by the side harmonic peaks in the case of Real(ε_M)= -1.5 and -3.0.

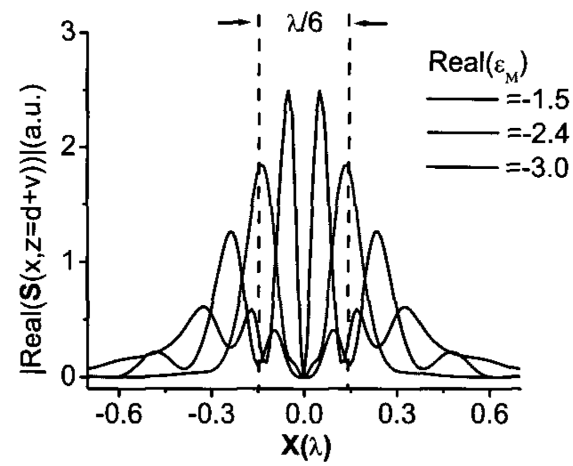

Fig. 3 The image collected at paraxial focal plane with the original sources separated by λ/6.

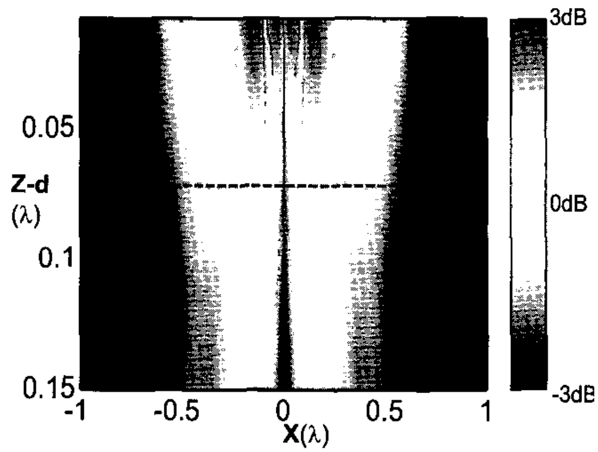

Fig. 4. The 3D log plot of power density |Real(S(x, z))| in medium 2 for the case of Fig. 3. The dashed line corresponds to the paraxial focal plane by geometric optics.

Finally, to record this near-field image, we have simulated the power density distribution in the medium ε2. In this case we select ε_M= -2.4, while other conditions remain unaltered as in Fig. 3. Counter-intuitively, we should not expect to have the highest power flux at focal point in the case of superlens imaging. The origin of this effect is connected to the decaying nature of evanescent field. In order to restore the strength of evanescent field at image plane, the field strength is indeed much higher at the surface of metamaterial slab. The elevated evanescent field strength at the exit of the superlens overweighs the contribution from propagating waves, so that the phase contour[8] instead of the power flux should be chosen as a measure in determination of focal plane.

V. Conclusion

In conclusion, we have established a model for asymmetric metamaterial superlens. The image transfer quality of the lens is characterized using Optical Transfer Function (OTF) of increasing spatial components. The simulation result demonstrated the restoration of evanescent field at imaging plane. It is found that the mismatch of dielectric properties and loss significantly reduced the minimum resolution of silver film lens. At wavelength 364nm (ε_M=-2.4+0.27i), the simulated resolution limit with 36nm film is ~λ/6. Simulation also revealed the possibility of obtaining reduction or magnification of features by tuning the working wavelength. Finally, because of elevated field amplitude at the exit surface of metamaterial slab, the 3D power flux in superlens is no longer a good measure to find the focal plane.

Acknowledgement

The authors are grateful to Dr. S. A. Ramakrishna and Prof. J. B. Pendry of Imperial College and Prof. D. Smith of UCSD for the helpful discussion. This work was supported by the MURI (Grant # N00014-01-1-0803), ONR (Grant # N00014-02-1-0224), and the NSF (Grant # DMII-9703426).

References

[1] Kosaka, H., Kawashima, T., et al, "Superprism Phenomena in Photonic Crystals", *Phys. Rev. B*, Vol 58, R10096, 1998.
[2] Smith, D., Padilla, W., et al, "Composite Medium with Simultaneously Negative Permittivity and Permeability", *Phys. Rev. Lett.*, Vol. 84, p4184, 2000.
[3] Shelby, R., Smith, D., and Schultz, S., "Experimental verification of a negative index of refraction", *Science*, Vol. 292, p77, 2001.
[4] Veselago, V., "The Electrodynamics of Substances with Simultaneously Negative ε and μ", *Sov. Phys. Usp.*, Vol.10, p509, 1968.
[5] Pendry, J.B., "Negative Refraction Makes a Perfect Lens", *Phys. Rev. Lett.*, Vol. 85, p3966, 2000.
[6] Notomi,M., "Theory of light propagation in strongly modulated photonic crystals: Refractionlike behavior in the vicinity of the photonic band gap", *Phys. Rev. B.*, Vol. 62, R10696, 2000.
[7] Raether, H., "Excitation of Plasmons and Interband Transitions by Electrons", Chap. 10, Springer Verlag, Berlin, 1980.
[8] Ziolowski, R. W., Heyman, E., "Wave propagation in media having negative permittivity and permeability", *Phys. Rev. E*, Vol. 64, R056625, 2001.
[9] Ramakrishna S. A., Pendry J. B., Schurig D., Smith D. R., Schultz. S., "The Asymmetric Lossy Near Perfect Lens", *J. Mod. Optics* (in press)
[10] Shamonina E., Kalinin V. A., Ringhofer K. H., Solymar L., "Imaging, compression and Poynting vector streamlines for negative permittivity materials", *Electron. Lett.*, Vol. 37, p1243, 2001.